PHYSICAL REVIEW E **78**, 040802(R) (2008)

Dynamics of polymer bridge formation and disruption

Joris Sprakel,[1,*] Erik Bartscherer,[2] Gerd Hoffmann,[2] Martien A. Cohen Stuart,[1] and Jasper van der Gucht[1]
[1]*Laboratory of Physical Chemistry and Colloid Science, Wageningen University, Dreijenplein 6, 6703 HB Wageningen, The Netherlands*
[2]*JPK Instruments AG Molecular Analytics, Tatzberg 47, 01307 Dresden, Germany*
(Received 8 July 2008; published 23 October 2008)

In this Rapid communication, we show, with colloidal probe atomic force microscopy(AFM) measurements, that the formation and subsequent disruption of polymer bridges between two solid surfaces is characterized by slow relaxation times. This is due to the retardation of polymer dynamics near a surface. For colloidal particles that are in constant (Brownian) motion kinetic aspects are key. To understand these effects, we develop a model of polymer bridging and bridge disruption that agrees quantitatively with our experiments.

DOI: 10.1103/PhysRevE.78.040802 PACS number(s): 82.35.Gh, 07.10.Pz, 82.70.Dd

Polymers can induce attractive interactions between two surfaces [1]. The best-known examples are perhaps the depletion attraction for nonadsorbing polymers [2] and the bridging attraction for adsorbing polymers [3,4]. Theories of bridging interactions often focus on thermodynamic equilibrium [1,5,6]. However, the dynamics of polymers near surfaces is often very slow [7], so that an equilibrium state may not be reached in practical cases. This can have great consequence for the interactions between colloidal particles that are in constant motion with respect to each other. To investigate such effects, we study the kinetics of bridge formation and disruption with colloidal probe atomic force microscopy (AFM). A simple kinetic model is developed that quantitatively describes the data and elucidates the molecular processes underlying the observed forces.

With the colloidal probe AFM technique [8], the interaction force F between a spherical particle and a planar solid surface is measured as a function of the separation distance h. An oxidized silicon wafer is employed as the flat substrate and a 3-μm-radius silica sphere as the colloidal probe, which is glued to a standard contact mode cantilever with a nominal spring constant of 0.06 N/m. The measurements are carried out on the ForceRobot (JPK Instruments), which is an automated AFM setup with built-in active vibration reduction. Actual spring constants of the cantilevers are measured with the thermal noise method [9]. Measurements consist of three stages: (I) compression (approach), (II) a contact (surface) delay of t_s seconds (ranging between 0 and 10 s), and (III) decompression (retraction). The velocity of (de)compression is set to $v=\pm 500$ nm/s, unless stated otherwise. For $t_s>0$, step II is activated with a repulsive trigger force on approach of 500 pN.

We study the bridging forces between adsorbed layers of telechelic associative polymers. The equilibrium bridging interactions between such layers have been predicted theoretically quite extensively, e.g., using the Milner-Witten-Cates self-consistent field formalism [5,6]. These telechelic polymers consist of a hydrophilic polymer [polyethylene oxide (PEO)], modified on both ends with an alkyl tail. In dilute aqueous solutions they form micelles, which are often called flowerlike micelles, due to the petal-like structure of the looped corona chains. When these micelles are brought close enough, polymeric bridges between them will be formed [11]. We use the following nomenclature for the polymers: Cm-pk, where m is the number of carbon atoms in the alkyl tails and p is the molecular weight (in kg/mol) of the water-soluble backbone, e.g., C14-20k is a PEO chain of 20 kg/mol modified with tetradecyl tails at both ends. The preparation of these polymers has been described elsewhere [10]. Prior to the measurements, the surfaces are submerged in a 0.1 g/l polymer solution in $10^{-2}M$ NaCl, and left to equilibrate for at least 1 h. During equilibration the micelles adsorb onto the solid silica surfaces with their PEO chains [12]. For these polymeric surfactants, the large head group (PEO part) leads to a large preference for spherically symmetric micelles. This shape is partly retained at the surface [13].

All measured $F(h)$ curves share two common features (Fig. 1): (i) on approach a purely repulsive force is found and (ii) on retraction an attractive well appears due to the formation of polymer bridges between the surface layers. The repulsive interaction on approach is partly electrostatic and partly steric in origin. In pure solvent, only the electrostatic component is observed (solid curve in Fig. 1), for which the Debye length $\kappa^{-1}=3$ nm. The additional repulsion in the

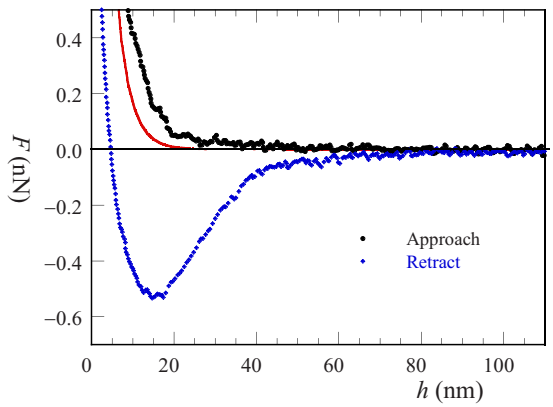

FIG. 1. (Color online) Typical force-separation curve for a full scan, showing the approach (●) and retraction (◆) traces, with $v=500$ nm/s, $t_s=1$ s for 0.1 g/l C16-20k. Drawn line shows an averaged approach trace for measurements in pure solvent ($10^{-2}M$ NaCl).

*Also at Dutch Polymer Institute (DPI), P. O. Box 902, 5600 AX Eindhoven, the Netherlands. Joris.Sprakel@wur.nl

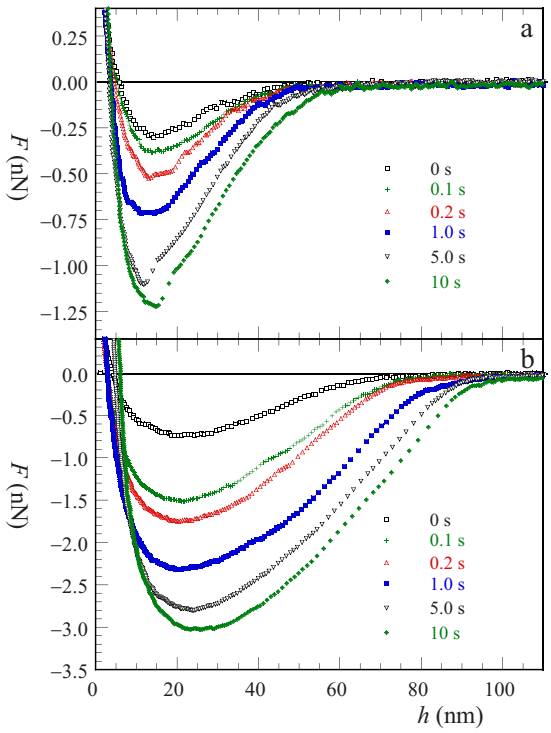

FIG. 2. (Color online) Retraction traces with varying surface delay times t_s, as indicated in the plots, recorded at $v=500$ nm/s for C16-20k (a) and C18-20k (b).

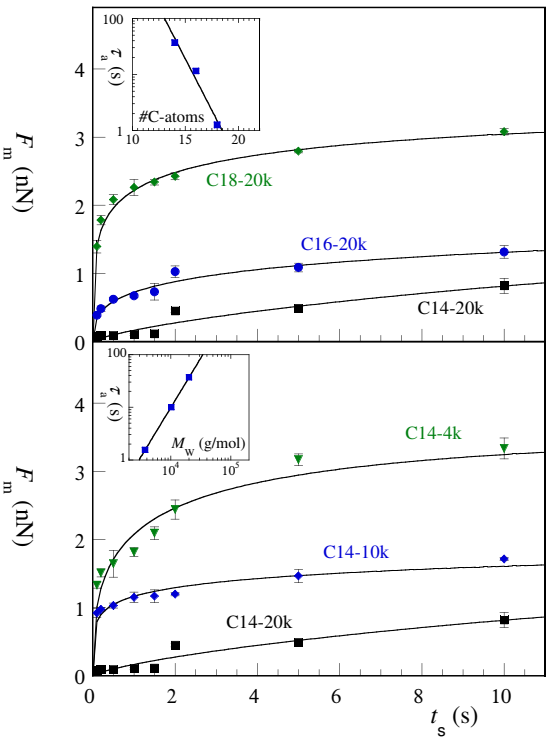

FIG. 3. (Color online) Absolute values of the maximum attractive force F_m versus surface delay times t_s, recorded at $v=500$ nm/s for (a) 20 kg/mol PEO end capped with alkyl tails of increasing length (C_{14},C_{16},C_{18}); (b) tetradecyl end capped PEO of varying molar weights (4, 10, and 20 kg/mol). Drawn lines are fits to Eq. (1). Insets shows the corresponding values of τ_a as a function of the number of carbon atoms in the alkyl tails (a) and polymer chain length (b).

polymer solutions is due to compression of the adsorbed polymers. It starts around 20 nm, corresponding to twice the hydrodynamic radius of the flowerlike micelles, $R_h=9.9\pm0.5$ nm, as found from light scattering. This indicates that the micellar structure is indeed largely preserved at the surface.

The hysteresis observed between approach and retraction in Fig. 1 already shows that the bridging process occurs on relatively long time scales. This is further confirmed when we change the time t_s that the surfaces are kept in contact (Fig. 2). We see that at the shortest surface delay time of $t_s=0$, corresponding to an effective contact time of approximately 40 ms, there is already a significant bridging attraction. When we increase the contact time, up to 10 s, the bridging force continues to increase. Longer delay times are not accessible due to physical limitations of the technique.

In Fig. 3, we plot the maximum attractive force F_m as a function of the surface delay time t_s. Assuming that the force, at a given surface separation h, is proportional to the number of bridges n_b, which we will justify below, Fig. 3 reflects the kinetics of bridge formation.

Figure 3 does not show a single exponential relaxation, hence the bridge formation is not a first-order process with a single relaxation time. The data can be fitted with a stretched exponential relaxation (Fig. 3):

$$F_m = F_{m,\infty}\left\{1-\exp\left[-\left(\frac{t_s}{\tau_a}\right)^{\beta}\right]\right\}, \qquad (1)$$

where τ_a is the average bridging time scale, $F_{m,\infty}$ is the final plateau in F_m, and β is the stretch exponent, here found to be approximately 1/2. The values of τ_a found by fitting the data to Eq. (1) are shown in the inset in Fig. 3 and are between 1 and 50 s. This is several decades larger than the bulk relaxation time for these polymers, which is on the order of 1 ms [14].

The reason for this slow bridge formation is that the PEO chains are partly adsorbed onto the silica surface. In order to form a bridge, segments must desorb, which is a slow process. Moreover, depending on the position of a chain with respect to the surface, the number of adsorbed segments, and consequently also the desorption rate, can vary. This would lead to a distribution of relaxation times, which explains the stretched exponential form [Eq. (1)].

The typical association time scale increases with polymer length [inset in Fig. 3(b)]. For polymer desorption, the energy barrier for desorption scales with the number of binding sites, which increases approximately as the radius of gyration of the polymer. We also find that τ_a decreases with the length of the alkyl tails [inset in Fig. 3(a)]. We attribute this to the fact that longer alkyl tails give a stronger driving force for micelle formation [11], and hence the micelles will be less deformed at the surface. This leads to a reduction of the number of segments per chains that are adsorbed onto the surface. As a result desorption will be faster for adsorbed layers formed from telechelic polymers with longer alkyl tails. Note that in bulk the relaxation time is an increasing function of alkyl length [14].

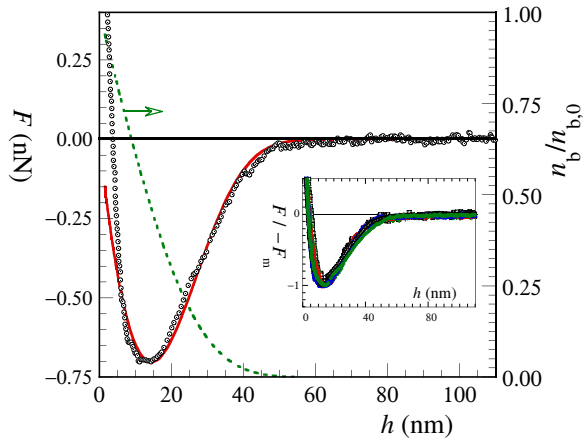

FIG. 4. (Color online) Comparison between the model [drawn line, Eq. (3)] and experimental data [●, as in Fig. 2(a) for t_s=1 s]. Fixed model parameters: N=225, l_K=0.9 nm, δ=2 nm, and v =500 nm/s. Fitted parameters: n_B=1600 and $k_{d,0}$=20.1 s^{-1}. Dotted line shows the corresponding relative change in the number of bridges, $n_b/n_{b,0}$. Inset presents same data as in Fig. 2(a), showing the force F scaled to the maximum attractive force F_m, collapsing $F(h)$ for various t_s onto a single curve.

The total number of bridges formed at very long contact times, represented by $F_{m,\infty}$, is found to decrease with polymer length and to increase with alkyl tail length. This is thought to be caused by changes in the surface coverage. Larger alkyl tails and shorter polymer backbones give larger micellar aggregation numbers [11], leading to increasing number of chains adsorbed per unit area.

Upon increase in the separation between the surfaces (retraction phase), the bridges that are present will be disrupted. To describe this process, we assume that the dissociation of bridges is a first-order reaction and that pulling on the chains enhances dissociation. Assuming that bridge disruption is an activated process, the dissociation rate is expected to increase exponentially with the pulling force f_b:

$$\frac{\partial n_b}{\partial t} = -k_d n_b = -k_{d,0} n_b \exp\left(\frac{f_b \delta}{k_B T}\right), \tag{2}$$

where $k_{d,0}$ is the rate constant when there is no force on the polymers and δ is the length over which the force acts (here the length of the alkyl tails). For the force per bridge we use a Gaussian spring approach, $f_b = 3vtk_BT/Nl_K^2$, where $h=vt$ and N is the number of statistical segments in the chain with Kuhn length l_K. The total force $F=f_b n_b$ can then be calculated as a function of the distance h:

$$F = \frac{3k_BThn_{b,0}}{Nl_K^2} \exp\left\{\frac{k_{d,0}Nl_K^2}{3v\delta}\left[1 - \exp\left(\frac{3\delta h}{Nl_K^2}\right)\right]\right\}, \tag{3}$$

where $n_{b,0}$ is the number of bridges at the beginning of the retraction. This result implies that the curves shown in Fig. 2 all have the same shape and differ only in $n_{b,0}$. Upon rescaling the curves with F_m, which is directly proportional to $n_{b,0}$, we can collapse all curves measured at a given v for various t_s, as shown in the inset in Fig. 4 for one data set.

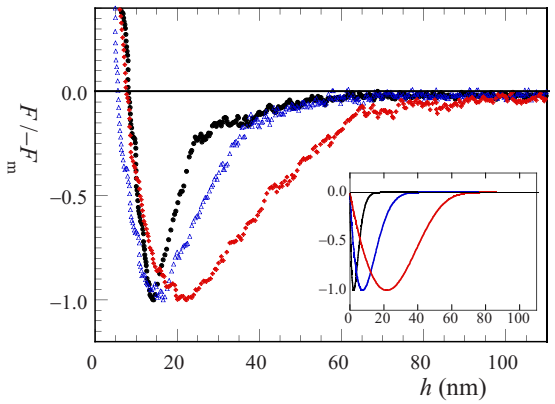

FIG. 5. (Color online) Effect of retraction velocity (v=50 ●, 200 △, and 1000 ♦ nm/s) on the force-distance profile, for C16-20k and t_s=0. Inset shows the corresponding prediction of our model [Eq. (3)], with the same parameters as in Fig. 4.

To compare Eq. (3) with our experiments, we enter realistic parameters in our model for the Kuhn length of PEO (l_K=0.9 nm [15]), the number of statistical segments (N =225 for PEO-20k) and the alkyl contour length ($\delta \approx 2$ nm for $C_{16}H_{33}$). To describe our data, we have now two remaining parameters, i.e., $n_{b,0}$ and $k_{d,0}$. In Fig. 4 we see that the model describes the experimental data very well. For this example, i.e., a C16-20k polymer and t_s=1 s, we find $n_{b,0}$ =1600 and $k_{d,0}$=20 s^{-1}.

During the retraction stage the force per bridge increases, while the number of bridges decreases (dotted line in Fig. 4), giving rise to the minimum in the force. Note that in the measurements, a short-ranged repulsive force is present, as discussed above, which is not accounted for in the model. This explains the deviations between experiment and model for short distances. We also assumed that all chains are elongated by the same amount; this is an approximation since the bead surface is curved.

We can estimate the total number of polymer chains between the interacting surfaces by assuming that bridges can form only in the region where the separation is less than 25 nm (i.e., less than $5R_g$). The surface area of a spherical cap, with base radius 3 μm and height 25 nm, is approximately 0.5 μm^2. From optical reflectometry measurements, we find an adsorbed amount of 1.8 mg/m^2. Combining these numbers leads to a estimated total of 10^4 polymer chains in the area of interaction. For a contact time of t_s=1 s, we found that 1600 bridges had been formed, which is roughly $\frac{1}{5}$ of the total number of polymer chains.

From Fig. 2 it can be seen that the range of the bridging attraction is larger for C_{18}-modified polymers than for those with C_{16} tails. The reason for this is that longer alkyl tails dissociate more slowly from the micelles than do short ones ($k_{d,0}$ is smaller and δ is larger), so that the chains can be stretched further before the bridges are disrupted. Similarly, the range is longer for polymers with a longer PEO spacer, because longer chains can be stretched further (data not shown).

The characteristic disruption time scale for the polymer in the example (C16-20k, Fig. 4), $\tau_{d,0}=1/k_{d,0} \approx 0.05$ s, whereas the time scale for association τ_a for the same polymer is

11.5 s. In bulk solution, the relaxation times for these processes are around 1 ms, again showing the large retardation of the polymers near solid surfaces. There clearly is an asymmetry between the time scales for bridge formation and disruption. Two reasons for this asymmetry come to mind. First of all, formation of the bridges takes place in a compressed configuration, leading to a high density of polymers in the gap between the surfaces that slows down the chain dynamics. Second, it is not hard to imagine that a loop configuration of the chain allows more segments to adsorb onto the surfaces than a bridge conformation, which in principle is directed normal to the surfaces. This also causes the kinetics of bridge disruption to be faster than that of bridge formation.

In colloidal systems, the velocity with which particles move is governed by their size and the viscosity of the surrounding medium. The relative velocity between two particles can therefore vary over many decades. We see that the separation velocity has a strong influence on the shape of the bridging attraction force (Fig. 5). When the separation velocity is increased, the position of the maximum attraction shifts to larger separations and the overall range of the bridging force increases. Both features are also predicted by our model [Eq. (3)], as shown in the inset in Fig. 5.

We conclude that the dynamics of polymer bridging can be understood with first-order association-dissociation reactions. Bridge formation is governed by a distribution of rate constants, while the disruption rate is increased by pulling the surfaces apart. The slow time constants for these processes indicate that these kinetic considerations are important for understanding the effect of polymer bridging on the interactions between "real" colloidal particles. Modeling the dynamics of these systems with a simple argument based on activated sticker extraction is a very versatile strategy. Recently, we have shown that it can also predict the nonlinear shear rheology of macroscopic networks of the same polymers [10].

The work of J.S. forms part of the research program of the Dutch Polymer Institute (DPI), Project No. 564.

[1] G. J. Fleer, M. A. Cohen Stuart, J. M. H. M. Scheutjens, T. Cosgrove, and B. Vincent, *Polymers at Interfaces* (Chapman & Hall, London, 1993).

[2] W. K. Wijting, W. Knoben, N. A. M. Besseling, F. A. M. Leermakers, and M. A. Cohen Stuart, Phys. Chem. Chem. Phys. **6**, 4432 (2004).

[3] M. Giesbers, J. M. Kleijn, G. J. Fleer, and M. A. Cohen Stuart, Colloids Surf., A **142**, 343 (1998).

[4] L. Cohen-Tannoudji, E. Bertrand, L. Bressy, C. Goubault, J. Baudry, J. Klein, J. F. Joanny, and J. Bibette, Phys. Rev. Lett. **94**, 038301 (2005).

[5] S. T. Milner and T. A. Witten, Macromolecules **25**, 5495 (1992).

[6] W. H. Tang and T. A. Witten, Macromolecules **29**, 4412 (1996).

[7] S. Sukhishvili, Y. Chen, J. D. Müller, E. Gratton, K. S. Schweizer, and S. Granick, Macromolecules **35**, 1776 (2002).

[8] W. A. Ducker, T. J. Senden, and R. M. Pashley, Nature **353**, 239 (1991).

[9] J. L. Hutter and J. Bechhoefer, Rev. Sci. Instrum. **64**, 1868 (1993).

[10] J. Sprakel, E. Spruijt, M. A. Cohen Stuart, N. A. M. Besseling, M. P. Lettinga, and J. van der Gucht, Soft Matter **4**, 1696 (2008).

[11] J. Sprakel, N. A. M. Besseling, M. A. Cohen Stuart, and F. A. M. Leermakers, Eur. Phys. J. E **25**, 163 (2008).

[12] B. R. Postmus, F. A. M. Leermakers, L. K. Koopal, and M. A. Cohen Stuart, Langmuir **23**, 5532 (2007).

[13] C. Ligoure, Macromolecules **24**, 2968 (1991).

[14] J.-F. Berret, D. Calver, and M. Viguier, Curr. Opin. Colloid Interface Sci. **8**, 296 (2003).

[15] S. Kawaguchi, G. Imai, J. Suzuki, A. Miyahara, and T. Kitano, Polymer **38**, 2885 (1997).